Effects of Spacer Length on the Side-Chain Micellization in Random Copolymers of Sodium 2-(Acrylamido)-2-methylpropanesulfonate and Methacrylates Substituted with Ethylene Oxide-Based Surfactant Moieties

Tetsuya Noda, Akihito Hashidzume, and Yotaro Morishima*

Department of Macromolecular Science, Graduate School of Science, Osaka University, Toyonaka, Osaka 560-0043, Japan

Received October 4, 2000; Revised Manuscript Received December 4, 2000

ABSTRACT: Side-chain micellization in the copolymers of sodium 2-(acrylamido)-2-methylpropanesulfonate and methacrylates substituted with $HO(CH_2CH_2O)_mC_{12}H_{25}$ ($C_{12}E_m$), where $m = 2$, 6, and 25, was investigated in 0.1 M NaCl aqueous solutions focusing on the effect of the ethylene oxide (EO) spacer length (m) on the apparent critical micelle concentration (cmc), aggregation number (N_{agg}) of the side-chain hydrophobes in polymer-bound micelles, hydrodynamic radius of polymer assemblies, steady-shear viscosity, and viscoelastic behavior. The cmc decreased with increasing m, an opposite trend to that of the corresponding free $C_{12}E_m$ surfactant molecules, whereas N_{agg} decreased with increasing m, a similar trend to that of the free surfactant molecules. N_{agg} values for the copolymers with $m = 6$ and 25 were virtually the same as those for micelles formed from free $C_{12}E_6$ and $C_{12}E_{25}$ molecules, respectively. Steady-shear viscosity increased gradually at low or intermediate polymer concentrations (C_p), followed by a drastic increase at higher C_p. Viscosities for the copolymers with $m = 25$ are roughly 2 and 3 orders of magnitude higher than those of the copolymers with $m = 6$ and 2, respectively, at a given C_p. Dynamic viscoelastic measurements revealed that the number density of mechanically active chains for the copolymer with $m = 25$ is roughly 1 and 4 orders of magnitude larger than those for the copolymers with $m = 6$ and 2, respectively, at a given C_p, indicating that interpolymer side-chain micellization occurs more favorably for the copolymer with longer EO spacer length leading to a network structure of a higher cross-linking density. The rheological terminal relaxation times decreased with increasing m, indicating that the lifetime of the transient network is shorter for larger m.

Introduction

The self-assembly of hydrophobically modified water-soluble polymers has been extensively studied in recent years because of their potential in industrial applications and also because of their relevance to biological macromolecular systems.[1−4] A large number of investigations have focused on hydrophobically modified polymers with various architectures, including amphiphilic polyelectrolytes. A characteristic feature of hydrophobic self-associations in amphiphilic polyelectrolytes is that the hydrophobic association competes with electrostatic repulsion, showing a marked tendency of preferential intra- or interpolymer association depending on macromolecular architectures.[5−17]

In the case of polymers substituted with hydrophobes in their side chains, spacer bonding between the hydrophobe and main chain has an important effect on the association of polymer-bound hydrophobes. Hwang and Hogen-Esch[18] have pointed out two conceivable effects of the spacer: (i) alleviation of an excluded-volume effect on interpolymer hydrophobic association with increased spacer length and (ii) "decoupling" of motions of the polymer chain and hydrophobes.

We previously investigated the association behavior of copolymers of sodium 2-(acrylamido)-2-methylpropanesulfonate (AMPS) and a methacrylate substituted with a nonionic surfactant moiety $HO(CH_2CH_2O)_{25}C_{12}H_{25}$ ($C_{12}E_{25}$) in 0.1 M NaCl aqueous solutions.[19] In this associative comonomer, a C_{12} chain is linked to a polymerizable methacrylate moiety via a $(CH_2CH_2O)_{25}$ spacer chain. The polymer-bound $C_{12}E_{25}$ surfactant moieties undergo micellization as if they were free surfactant molecules, forming micelles with aggregation numbers (N_{agg}) similar to those formed by free $C_{12}E_{25}$ surfactant molecules. This suggests that the hydrophilic $(CH_2CH_2O)_{25}$ spacer chain is flexible and long enough to decouple the motions of the polymer backbone and C_{12} chains attached to the other end of the $(CH_2CH_2O)_{25}$ spacer. In the copolymer, the surfactant moieties are held sufficiently close together on the same polymer chain, allowing them to assemble into a micelle within the same polymer molecule; but some surfactant groups on different polymer chains occupy the same micelle, and thereby polymer chains are cross-linked through micelles, forming a network structure.[19,20]

We extended the earlier study to a series of copolymers of AMPS and methacrylates substituted with $HO(CH_2CH_2O)_mC_{12}H_{25}$ ($C_{12}E_m$), where $m = 2$, 6, and 25, with varying contents of the associative comonomers. The objectives of the present work are twofold: (i) to investigate the effect of the ethylene oxide (EO) spacer length on the micellization of surfactant moieties linked as side chains to the polyelectrolyte and (ii) to characterize rheological properties of polymer-bound micelle solutions as a function of the EO spacer length. Fluorescence techniques were used to determine apparent critical micelle concentration (cmc) and N_{agg} of the hydrophobes. Quasielastic light scattering (QELS) was employed to determine the hydrodynamic radius (R_h) of polymer assemblies formed as a result of interpolymer side-chain micellization at dilute and semidilute polymer concentrations.

10.1021/ma0017283 CCC: $20.00
Published on Web 02/02/2001

Similar associative comonomers consisting of an EO chain as the spacer between a polymerizable moiety at one end and a terminal hydrophobe at the other end have been employed for preparation of hydrophobically associative thickeners (AT polymers) by copolymerizing with water-soluble monomers such as acrylamide[18,21] and (meth)acrylic acid.[22−25] In this type of AT polymers, polymer-bound hydrophobes act as "stickers", leading to a physically cross-linked structure. The contents of associative comonomers in such AT polymers are normally less than 2 mol %, which is enough to result in a sufficient degree of cross-links necessary for AT polymers. Different from these conventional AT polymers, a feature of the copolymers in the present work is that a much larger number of surfactant comonomer units are incorporated into a strong polyelectrolyte, allowing the polymer-bound surfactant moieties to undergo side-chain micellization rather than to act simply as stickers.

Experimental Section

Materials. Nonionic surfactants, di- and hexaethylene glycol mono-*n*-dodecyl ether ($C_{12}E_2$ and $C_{12}E_6$, respectively) and poly(ethylene oxide) mono-*n*-dodecyl ether, of number-average degree of polymerization of 25 ($C_{12}E_{25}$), and 2-(acrylamido)-2-methylpropanesulfonic acid (AMPS), were purchased from Wako Pure Chemical Co. and used without further purification. Methacryloyl chloride (Wako Pure Chemical Co.), benzene, and *N*,*N*-dimethylformamide (DMF) were distilled under reduced pressure over calcium hydride. 2,2′-Azobis(isobutyronitrile) (AIBN) was recrystallized from ethanol. Pyrene was recrystallized twice from ethanol. Water was purified with a Millipore Milli-Q system. Other reagents were used as received.

Associative Monomers. Methacrylates substituted with $HO(CH_2CH_2O)_mC_{12}H_{25}$ ($C_{12}E_m$), where $m = 2$ and 6 (abbreviated as DE2MA and DE6MA, respectively), were synthesized following the procedure for the preparation of a methacrylate substituted with $HO(CH_2CH_2O)_{25}C_{12}H_{25}$ (DE25MA) reported previously.[19] Yields of DE2MA and DE6MA were 50.9% and 75.2%, respectively.

Polymers. Copolymers of AMPS and DE*m*MA ($m = 2$, 6, and 25) were prepared by free radical copolymerization in the presence of AIBN in DMF at 60 °C. A representative polymerization procedure is as follows: A known amount of AMPS was neutralized by equinormal of Na_2CO_3 in DMF, and a predetermined amount of DE2MA, DE6MA, or DE25MA and AIBN was added to this solution. The mixture of the monomers and the initiator was placed in a glass ampule and outgassed on a high-vacuum line by six freeze−pump−thaw cycles. The ampule was then sealed under high vacuum. Polymerization was carried out at 60 °C for 24 h. The polymerization mixture was poured into a large excess of diethyl ether to precipitate polymers. The polymer was purified by reprecipitation from methanol into a large excess of diethyl ether three times and then dissolved in pure water. The aqueous solution was dialyzed against pure water for a week using a cellulose tube (Viskase Sales Co., pore size: 36/32, corresponding to a cutoff molecular weight of 12 000−14 000). Polymers were recovered by a freeze-drying technique. The compositions of the copolymers were determined by ^{1}H NMR spectroscopy as reported previously.[19]

Measurements. a. NMR. ^{1}H NMR spectra of the associative comonomers were measured with a JEOL GSX-400 NMR spectrometer in $CDCl_3$ at 30 °C. ^{1}H NMR spectra of the copolymers were measured on the same spectrometer using D_2O as solvent at 60 °C. Chemical shifts were determined using TMS as an internal standard.

b. Gel Permeation Chromatography (GPC). GPC measurements were performed at 40 °C with a JASCO GPC-900 system equipped with an Asahipak GF-7M HQ column (Shodex) in combination with JASCO UV-975 (at 290 nm) and RI-930 detectors. A 0.1 M $LiClO_4$ methanol solution was used as eluent with an elution rate of 1.0 mL/min. Molecular weights of polymers were calibrated with standard poly(ethylene glycol) samples (Scientific Polymer Products, Inc.).

c. Absorption Spectra. Absorption spectra were recorded on a JASCO V-550 spectrophotometer using a 1.0 cm path length quartz cuvette. The concentration of pyrene solubilized in the presence of the polymer was calculated from the absorbance at 338 nm using the molar extinction coefficient $\epsilon_{338} = 37\,000\ M^{-1}\ cm^{-1}$.[26]

d. Fluorescence. *(1) Steady-State Fluorescence Measurements.* Steady-state fluorescence spectra were recorded on a Hitachi F-4500 fluorescence spectrophotometer. Emission spectra of pyrene were measured with excitation at 337 nm at room temperature. Excitation spectra were monitored at 372 nm. The slit widths for both the excitation and emission sides were maintained at 2.5 nm during measurements. Sample solutions were prepared by dissolving a predetermined amount of polymer in an aqueous pyrene solution of a known concentration, and the solutions were allowed to stand for 1 day for equilibration. Aqueous pyrene solutions of given concentrations were prepared by diluting pyrene-saturated water as reported previously.[15,19]

For the determination of the critical micelle concentration (cmc) of the polymer, excitation spectra of pyrene were measured at varying concentrations of the polymer following the method reported by Wilhelm et al.[27]

(2) Time-Resolved Fluorescence Measurements. Fluorescence decay data were collected on a HORIBA NAES 550 system equipped with a flash lamp filled with H_2. Sample solutions containing pyrene as a fluorescence probe were excited at 337 nm, and pyrene fluorescence was monitored at 400 nm with a band-pass filter (Toshiba KL-40) and a cutoff filter (Toshiba L-38) placed between the sample and detector. Sample solutions were purged with Ar for about 30 min prior to measurement. Measurements were performed with a pyrene concentration of 1×10^{-7} M. The observed decay is a convolution of the sample decay function and the instrumental response function.[15,19]

The aggregation number (N_{agg}) of the polymer hydrophobes was determined by using pyrene as a fluorescence probe. Pyrene molecules were solubilized in polymer micelles at a high concentration such that excimer was formed within the micelle. Sample solutions were prepared by adding a small amount of a concentrated pyrene solution in acetone into aqueous solutions of the polymer. The determination of N_{agg} is based on the kinetic model proposed by Infelta[28a,c] and Tachiya[28b,d] for fluorescence quenching in monodisperse surfactant micellar systems.[29] In the present study, the excimer formation among pyrene molecules, resulting in the quenching of pyrene monomer fluorescence, was used to determine N_{agg}. Fluorescence decay data were fitted to the following equation, assuming that the distribution of fluorescence probe molecules over the micelles obeys a Poisson distribution.

$$\ln[I(t)/I(0)] = A_3[\exp(-A_4 t) - 1] - A_2 t \quad (1)$$

$$A_2 = k_0 + n_Q k_Q k^-/(k_Q + k^-) \quad (2a)$$

$$A_3 = n_Q k_Q{}^2/(k_Q + k^-)^2 \quad (2b)$$

$$A_4 = k_Q + k^- \quad (2c)$$

Here, $I(t)$ and $I(0)$ are the fluorescence intensities at time t and 0 following pulse excitation, respectively, k_Q is the pseudo-first-order rate constant for quenching of the excited probe, k_0 ($=\tau_0^{-1}$) is the fluorescence decay rate constant for pyrene inside the micelle without excimer formation, and n_Q is the average number of quenchers dissolved in a micelle, which is also expressed as $[Q]_m/[M]$ ($[Q]_m$ is the molar concentration of quencher inside micelle, and [M] is the molar concentration of micelles). k^- is the first-order rate constant for exit of pyrene molecules from a micelle. Because the quenching of pyrene monomer fluorescence is due to the excimer formation of

Chart 1. AMPS−DE*m*MA Copolymers

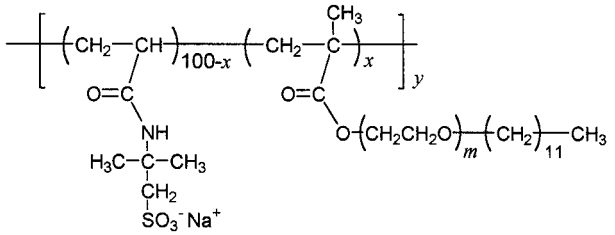

$m = 2$, $x = 1$, 10, and 15 — AMPS-DE2MA
$m = 6$, $x = 1$, 5, 10, and 20 — AMPS-DE6MA
$m = 25$, $x = 1$, 3, 5, 7, 10, 15, 20, and 30 — AMPS-DE25MA

pyrene in this study, $[Q]_m$ corresponds to the concentration of pyrene in the micelle. The $[Q]_m/[M]$ ratio ($=n_Q$) was determined from the best fit. N_{agg} is calculated from thus determined $[Q]_m/[M]$ ratio, as reported in detail in an earlier paper.[15]

e. Quasielastic Light Scattering (QELS). The apparent hydrodynamic radius (R_h) and the distribution of the relaxation times were measured with an Otsuka Electronics Photal DLS-7000 light scattering spectrometer equipped with a 65 mW Ar ion laser operating at $\lambda = 488$ nm. Data were collected using an ALV-5000 wide-band multi-τ digital autocorrelator. All measurements were performed at 25 °C. R_h and the distributions of relaxation times for polymer assemblies were measured varying the polymer concentration and scattering angle. Sample solutions were filtered prior to measurement using a 0.45 μm pore size disposable membrane filter. All the solutions were prepared in 0.1 M NaCl. To obtain the relaxation time distribution, the inverse Laplace transform analysis was performed by conforming the REPES algorithm.[30,31] Apparent values of R_h were calculated using the Einstein−Stokes relation. The details of the QELS measurement and data analysis have been reported elsewhere.[30−34]

f. Rheological Measurements. The rheological behavior of the copolymers was measured on a DynAlyser 100 stress-control rheometer (RheoLogica) equipped with a cone and plate at 25 °C. The radius of the cone is 40 mm, and the angle between the cone and plate is 4.0°. Steady shear and oscillatory flow measurements were conducted to obtain the steady shear viscosity and dynamic viscoelastic properties of polymer solutions. The values of the stress amplitude were checked to ensure that all experiments were performed within the linear viscoelastic regime, where the dynamic storage modulus (G') and loss modulus (G'') are independent of the applied stress.

Results

Characterization of Copolymers. Associative comonomers employed in the present work, methacrylates substituted with $HO(CH_2CH_2O)_mC_{12}H_{25}$ ($C_{12}E_m$), are abbreviated as DE*m*MA, where $m = 2$, 6, and 25 (Chart 1). The contents of the DE*m*MA units (f_{DEm}) in the copolymers were determined from ^{1}H NMR spectra in D_2O at 60 °C on the basis of the ratio of the area intensities of resonance peaks at 1.0 and 3.5 ppm due to methyl and methylene protons in the DE*m*MA and AMPS units, respectively.[19] The copolymer compositions were found to be practically the same as those in the monomer feed, which is an indication of random distribution of DE*m*MA units in the copolymers. In Table 1, f_{DEm} values for the copolymers used in this work are listed, the highest f_{DEm} values for copolymers with $m =$ 2, 6, and 25 being 15, 20, and 30 mol %, respectively. We also prepared copolymers with DE*m*MA contents higher than these f_{DEm} values, but solid polymer samples were found to be insoluble in water.

The molecular weights of the copolymers were roughly estimated by GPC calibrated with standard poly(ethylene glycol) samples using methanol containing 0.10 M $LiClO_4$ as an eluent (Table 1). In a separate study, weight-average molecular weights (M_w) obtained from static light scattering (SLS) measurements in methanol containing 0.10 M $LiClO_4$ were found to be close to the values estimated by GPC. Since we needed to know the number-average molecular weight (M_n) for the calculation of the number of side-chain $C_{12}E_m$ surfactant units per polymer chain, we used GPC for a rough estimation of M_n. M_w exhibits a tendency to increase with increasing f_{DEm}, molecular weight distributions (M_w/M_n) ranging from 1.5 to 3.0. From f_{DEm} and M_n, the number of DE*m*MA units per polymer chain was roughly calculated for each copolymer as listed in Table 1.

Table 1. Characteristics of AMPS−DE*m*MA Copolymers

comonomer	mol %[a]	M_w[b] (10^4)	M_w/M_n[b]	no. of $C_{12}E_m$ per polymer chain	cmc[c] (g/L)	K_v[c]
DE2MA	1	3.4	1.5	1.0	8.0	3.1×10^3
	10	5.6	1.5	10	2.3×10^{-2}	5.1×10^4
	15	6.9	1.8	23	1.6×10^{-2}	9.4×10^5
DE6MA	1	3.1	2.0	0.7	2.8	4.3×10^3
	5	5.0	2.2	4.1	9.3×10^{-2}	2.8×10^4
	10	4.8	2.4	6.5	1.2×10^{-2}	8.1×10^4
	20	6.9	2.7	17	2.2×10^{-2}	1.3×10^5
DE25MA	1	3.7	1.8	0.8	1.3	1.4×10^4
	3	3.1	3.0	1.2	3.6×10^{-1}	3.0×10^4
	5	5.6	2.9	3.5	1.3×10^{-1}	6.7×10^4
	7	6.1	2.9	5.9	5.6×10^{-2}	7.2×10^4
	10[d]	7.0	3.0	7.0	6.0×10^{-3}	1.1×10^5
	15[d]	6.9	1.9	13	1.8×10^{-2}	1.0×10^5
	20[d]	7.6	2.9	15	2.1×10^{-2}	1.1×10^5
	30[d]	8.3	2.8	16	2.4×10^{-2}	1.2×10^5

[a] Mole percent content of the comonomer in the copolymer determined by ^{1}H NMR in D_2O. [b] Determined by GPC using a 0.1 M $LiClO_4$ methanol solution as eluent. Standard poly(ethylene oxide) samples were used for the calibration of the molecular weight. [c] Determined from steady-state fluorescence excitation spectra of pyrene probes (see text). [d] Previously reported.

Hydrophobic Microdomains Formed by Polymer-Bound Dodecyl Groups. In AMPS−DE*m*MA copolymers, dodecyl groups may associate within the same polymer chain (intrapolymer association) and between different polymer chains (interpolymer association). We previously reported that AMPS−DE25MA copolymers showed an apparent critical micelle concentration (cmc) corresponding to the onset of interpolymer association in aqueous solution.[19] The apparent cmc for polyAMPS-bound $C_{12}E_{25}$ surfactant moieties was estimated using fluorescence excitation spectra of pyrene probes.[19] This method is based on the fact that the 0−0 absorption maximum for pyrene in water at 334 nm shifts to 337 nm when pyrene is solubilized in a micellar phase.[35] The ratio of the intensity at 337 nm relative to that at 334 nm (I_{337}/I_{334}), estimated from excitation spectra, increases with polymer concentration (C_p).[27] Figure 1 shows an example of excitation spectra for pyrene probes solubilized in aqueous solutions of the AMPS-DE6MA copolymer with $f_{DE6} = 20$ mol % at different C_p. It can be seen that the intensity at 337 nm increases with increasing C_p. From I_{337}/I_{334} at a given C_p, along with minimum and maximum I_{337}/I_{334} values observed at low and high C_p, respectively, one can calculate a ratio of pyrene concentrations in the micellar and aqueous phases ($[Py]_m/[Py]_w$) at a given C_p following the method reported in the literature.[27] Figure 2 shows plots of $[Py]_m/[Py]_w$ as a function of C_p for the AMPS−DE6MA copolymers with $f_{DE6} = 10$ and 20 mol %. The plots comprise two linear lines with a smaller slope at lower

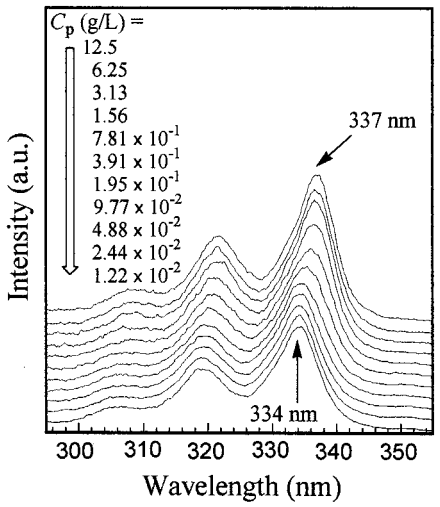

Figure 1. Steady-state fluorescence excitation spectra monitored at 338 nm for pyrene probes in 0.1 M NaCl aqueous solutions in the presence of varying concentrations of the copolymer with $f_{DE6} = 20$ mol %; [pyrene] = 1.0×10^{-7} M.

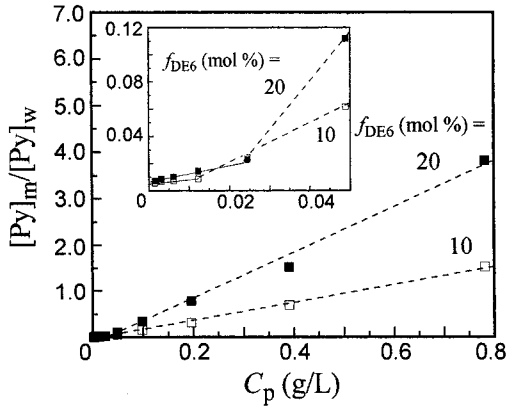

Figure 2. Plots of $[Py]_m/[Py]_w$ estimated from the I_{337}/I_{334} ratio against the polymer concentration for the copolymer with $f_{DE6} = 10$ and 20 mol % in 0.1 M NaCl aqueous solutions. The inset shows plots for a low-C_p region on an expanded scale.

C_p (inset in Figure 2) and a larger slope at higher C_p. The transition from the small to large slope is sufficiently abrupt to be able to define an apparent cmc, i.e., the onset of interpolymer hydrophobic associations. At low C_p, the polymer-bound surfactant moieties associate within the same polymer chain independent of C_p, forming intrapolymer hydrophobic domains. Upon an increase in C_p to a certain level, however, interpolymer association commences to occur. From a break observed in the $[Py]_m/[Py]_w$ vs C_p plot, apparent cmc was estimated, as listed in Table 1. The slope of the linear line corresponds to a partition coefficient (K_v) for pyrene solubilization; the steeper the slope, the stronger ability to solubilize pyrene in the micellar phase.[19] Micelles formed at $C_p >$ cmc are very different from intrapolymer hydrophobic domains formed at $C_p <$ cmc in ability to solubilize pyrene, probably because of a difference in the size of hydrophobic cores (i.e., aggregation number).

Measurements were also made for AMPS−DE2MA and AMPS−DE25MA copolymers ($f_{DE25} < 10$ mol %) with varying f_{DE2} and f_{DE25}, respectively, to determine apparent cmc and K_v values. Results are summarized in Table 1 and plotted in Figure 3 as a function of the comonomer content in the copolymer. Apparent cmc and K_v values for AMPS−DE25MA copolymers ($f_{DE25} \geq 10$ mol %) reported in our earlier paper[19] are also plotted

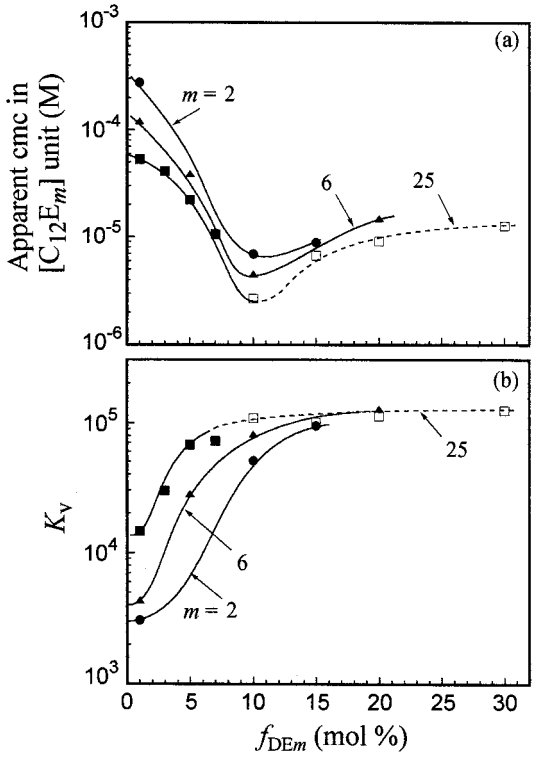

Figure 3. Plots of apparent cmc in terms of the molar concentration of the surfactant units (a) and the partition coefficient (K_v) for pyrene probes (b) as a function of f_{DEm}; (□) data reported in our previous paper.[19]

in Figure 3 for comparison. Figure 3a shows plots of apparent cmc values for the copolymers with $m = 2$, 6, and 25 as a function of the comonomer content in the copolymer. As m increases from 2 to 25, the apparent cmc decreases. For example, in the case of the copolymers with $f_{DEm} = 10$ mol %, cmc decreases from 7.2×10^{-6} M ($m = 2$) to 2.5×10^{-6} M ($m = 25$). This tendency is opposite to a general tendency observed for free $C_{12}E_m$ surfactant molecules.

In Figure 3a, with increasing f_{DEm} up to 10 mol %, the apparent cmc values for the copolymers with $m =$ 2, 6, and 25 decrease by more than 1 order of magnitude. However, a further increase in f_{DEm} beyond 10 mol % causes a gradual increase in cmc. It should be noted here that the apparent cmc values for the copolymers with varying f_{DEm} (except for $f_{DE6} = 1$ mol %) are smaller than those for the corresponding free $C_{12}E_m$ surfactants: 8.5×10^{-5} M for $C_{12}E_6$[36] and 2.8×10^{-4} M for $C_{12}E_{25}$ which we determined previously.[19]

K_v values estimated from Figure 2 are plotted in Figure 3b as a function of f_{DEm}. As the spacer length is increased, K_v increases when compared at the same content of the associative comonomer. For example, at $f_{DEm} = 10$ mol %, K_v increases from 5.1×10^4 ($m = 2$) to 1.1×10^5 ($m = 25$). Furthermore, K_v increases with increasing f_{DEm} at low f_{DEm}, reaching a maximum at $f_{DEm} > 15$ mol %. The maximum values for the AMPS−DE6MA and AMPS−DE25MA copolymers are slightly smaller than those of the corresponding free surfactants: 1.0×10^5 for $C_{12}E_6$ and 1.7×10^5 for $C_{12}E_{25}$, which were determined using the same fluorescence technique as described above.

Aggregation Number (N_{agg}) of Polymer-Bound Hydrophobes. We determined N_{agg} of dodecyl groups in the copolymers using a fluorescence technique based on the excimer formation of pyrene probes[37,38] solubi-

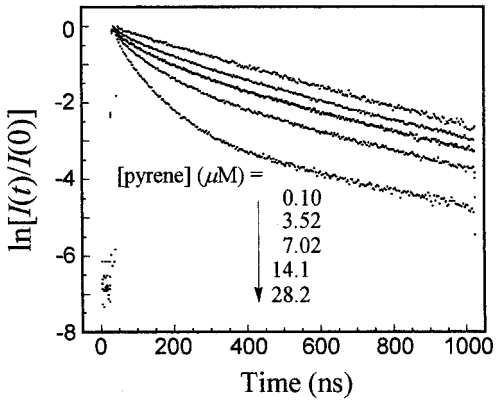

Figure 4. Comparison of fluorescence decays at different concentrations of pyrene probes in the presence of the copolymer with $f_{DE6} = 20$ mol % in 0.1 M NaCl aqueous solutions; $C_p = 6.25$ g/L.

lized in hydrophobic microdomains (micelle cores) formed from the AMPS−DE*m*MA copolymers. Figure 4 shows examples of fluorescence decay data for pyrene probes with different concentrations of pyrene solubilized in a 0.10 M NaCl aqueous solution in the presence of the AMPS−DE6MA copolymer with $f_{DE6} = 20$ mol % at $C_p = 6.25$ g/L. When the concentration of solubilized pyrene is very low, such that each micelle core contains much less than one pyrene molecule on average, pyrene monomeric fluorescence decays are single-exponential because no excimer is formed. As the pyrene concentration is increased, the probability of finding two or more pyrene molecules in the same micelle core increases, and pyrene monomeric fluorescence is quenched due to excimer formation, showing a fast decay component as can be seen in Figure 4. The fluorescence decay profiles were able to be best-fitted to a kinetic model (eq 1) proposed by Infelta[28a,c] and Tachiya[28b,d] wherein distributions of fluorophores and quenchers over the micelles are assumed to obey a Poisson distribution.

We performed fluorescence decay measurements for the AMPS−DE2MA copolymers with $f_{DE2} = 10$ and 15 mol % and AMPS−DE6MA copolymers with $f_{DE6} = 10$ and 20 mol % at several different concentrations of the polymer and pyrene. Some examples of fitting parameters for the AMPS−DE6MA copolymer with $f_{DE6} = 10$ mol % obtained from the best-fit of fluorescence decay data to eqs 1 and 2 are listed in Table 2. The average number of pyrene molecules solubilized in a micelle, n_Q, can be calculated from these parameters as

$$n_Q = (A_3A_4 + A_2 - k_0)^2/A_3A_4^2 \qquad (3)$$

From n_Q thus calculated, N_{agg} of hydrophobes in a micelle core can be calculated.[15] Fluorescence decay data for a low concentration of pyrene (1.0×10^{-7} M) at $C_p = 0.195-12.5$ g/L were confirmed to be single-exponential with a τ_0 value of ca. 380 ns for all the copolymers independent of the surfactant comonomer content. As can be seen in Table 2, A_2^{-1} values are practically the same as the τ_0 value (ca. 380 ns), indicative of the contribution of the second term in eq 2a being very small. A similar tendency was observed for the AMPS−DE6MA copolymer with $f_{DE6} = 20$ mol % and AMPS−DE2MA copolymers with $f_{DE2} = 10$ and 15 mol %. As can be seen in Table 2, there is no systematic change in A_4 with changes in both the polymer and pyrene concentrations. Values of n_Q calculated from eq 3 were found to be practically the same as the values of A_3, indicating that k^- is much smaller than k_Q (eq 2b).

Table 2. Fitting Parameters for Eq 1 and Aggregation Numbers of C_{12} Hydrophobes for the AMPS−DE6MA Copolymer with $f_{DE6} = 10$ mol %

C_p (g/L)	[pyrene][a] (μM)	A_3	$10^{-6}A_4$ (s^{-1})	A_2^{-1} (ns)	χ^2	N_{agg}
12.5	53.8	2.66	27.4	381	1.22	241
	26.9	1.35	28.6	377	1.32	246
	13.4	0.689	25.6	383	1.27	251
6.25	26.8	2.42	26.5	378	1.26	249
	13.4	1.29	29.2	378	1.33	254
	6.92	0.613	28.2	380	1.15	239
3.13	12.4	2.18	29.4	382	1.31	244
	6.18	1.14	25.7	374	1.27	263
	3.09	0.58	27.3	386	1.19	262
1.56	8.48	3.12	30.1	379	1.26	223
	4.21	1.56	28.1	378	1.12	233
	2.09	0.788	30.3	374	1.14	231
0.781	4.68	3.40	26.2	362	1.35	220
	2.33	1.69	27.0	371	1.39	209
	1.12	0.853	29.5	364	1.16	231
0.391	2.61	3.53	30.3	376	1.08	204
	1.34	1.32	30.4	374	1.19	175
	0.782	0.814	28.4	369	1.27	181
0.195	1.28	3.36	30.5	365	1.23	179
	0.687	1.59	32.4	370	1.29	183
	0.356	0.734	28.2	362	1.31	179

[a] Concentrations of pyrene were calculated from the absorbance at 338 nm using $\epsilon_{338} = 37\,000$ M^{-1} cm^{-1}.[26]

Figure 5a,b shows the plots of mean N_{agg} values thus estimated as a function of the molar concentrations of the $C_{12}E_6$ and $C_{12}E_2$ residues in the AMPS−DE6MA and AMPS−DE2MA copolymers, respectively, converted from C_p for the copolymers with varying contents of the surfactant comonomers. In Figure 5a, mean N_{agg} values for free $C_{12}E_6$ surfactants in 0.1 M NaCl aqueous solutions determined by the same fluorescence method are also plotted against the surfactant concentration. As can be seen from Figure 5a, N_{agg} values for the AMPS−DE6MA copolymers with $f_{DE6} = 10$ and 20 mol % slightly increase with increasing C_p in a low-C_p region ([$C_{12}E_6$ unit] $< 10^{-3}$ M) independent of f_{DE6} and level off at higher polymer concentrations. On the other hand, N_{agg} observed for free $C_{12}E_6$ surfactants increases over the concentration range studied, as compared in Figure 5a. N_{agg} values for the polymers and the free surfactant are nearly the same in the range 5×10^{-4} M < [$C_{12}E_6$ unit] $< 1 \times 10^{-3}$ M. Values of N_{agg} for the AMPS−DE2MA copolymers with $f_{DE2} = 10$ and 15 mol % are much larger than those for the AMPS−DE6MA copolymers with $f_{DE6} = 10$ and 20 mol % (Figure 5b), showing a similar dependence on the polymer concentration as the AMPS−DE6MA copolymers. We cannot compare these N_{agg} values with those of free $C_{12}E_2$ molecules because $C_{12}E_2$ is insoluble in water.

A large effect of the EO spacer length (i.e., *m*) on N_{agg} can be seen in Figure 6 where N_{agg} values for the AMPS−DE*m*MA copolymers with $f_{DEm} = 10$ mol % are plotted as a function of *m*. As *m* increases, N_{agg} decreases greatly, a trend similar to that of free $C_{12}E_m$ surfactants.

In the case of the AMPS−DE6MA copolymers, the numbers of polymer chains that constitute one micelle unit are calculated to be at least 29 and 10 for $f_{DE6} = 10$ and 20 mol %, respectively, from N_{agg} and the average numbers of surfactant comonomer units per polymer chain (Table 1). In the same manner, the numbers of polymer chains constituting one micelle unit

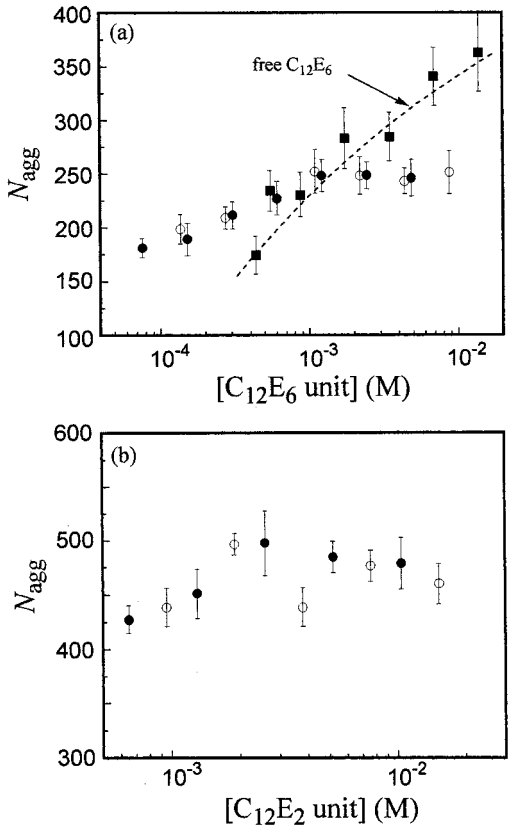

Figure 5. Dependence of N_{agg} on the molar concentration of the surfactant unit for the AMPS−DE6MA (a) and AMPS−DE2MA (b) copolymers with varying f_{DEm} in 0.1 M NaCl aqueous solutions: (a) f_{DE6} = 10 (○) and 20 (●) mol %; N_{agg} values for free $C_{12}E_6$ surfactants are also plotted (■); (b) f_{DE2} = 10 (○) and 15 (●) mol %. Experimental scatters are shown as error bars.

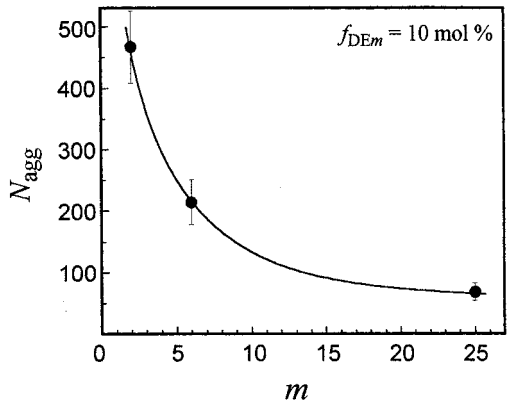

Figure 6. Relationship between N_{agg} and m for the copolymers with 10 mol % surfactant comonomer content in 0.1 M NaCl aqueous solutions.

for the AMPS−DE2MA copolymer are calculated to be at least 44 and 18 for f_{DE2} = 10 and 15 mol %, respectively. Thus, it is obvious that each micelle is formed from not only intrapolymer associations but also a large number of interpolymer associations, yielding a cross-linked structure.

For all the copolymers with lower f_{DEm} no quenching of pyrene monomeric fluorescence due to excimer formation was observed in the decay of monomeric pyrene fluorescence. This is probably because the ability of hydrophobic microdomains to solubilize pyrene is too low for the copolymers with lower f_{DEm}.

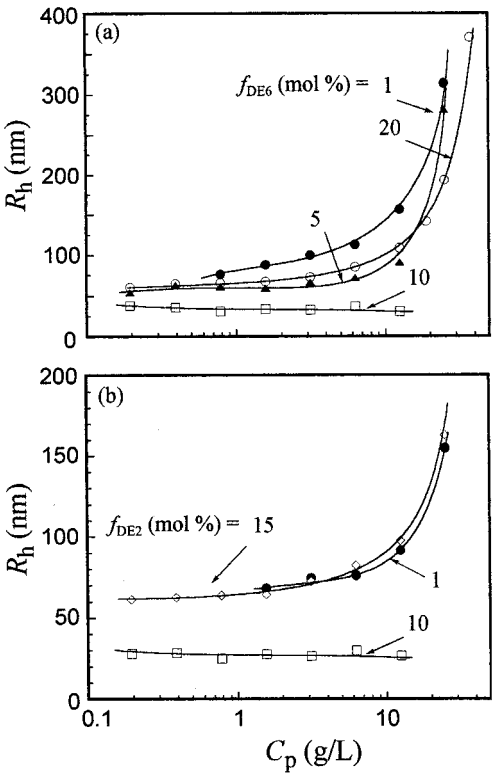

Figure 7. Dependence of R_h on C_p for the AMPS−DE6MA (a) and AMPS−DE2MA copolymers (b) with varying f_{DEm}.

Hydrodynamic Size of the Polymer Micelles. QELS measurements were carried out at several different scattering angles (50°−150°), and the field autocorrelation functions thus obtained were analyzed by using REPES.[30,31] Relaxation time distributions for the AMPS−DE2MA and AMPS−DE6MA copolymers were found to be bimodal except for the copolymers with f_{DEm} = 10 mol %, which exhibited unimodal distributions. We plotted the relaxation rates (Γ) (i.e., the reciprocal of the relaxation time) for the fast and slow modes as a function of the square of the scattering vector (q^2). The plots for the polymers in the C_p range of 0.195−25 g/L yielded straight lines passing through the origin (data not shown). These results indicate that both the fast and slow relaxation modes are due to translational diffusion of scatterers. From the diffusion coefficients (D) estimated from the slope of the $\Gamma-q^2$ plot, apparent hydrodynamic radii (R_h) corresponding to the fast and slow relaxation modes were calculated using the Einstein−Stokes relation.

In Figure 7, R_h values thus estimated for the slow relaxation mode for the AMPS−DE6MA and AMPS−DE2MA copolymers are plotted as a function of C_p. Values of R_h for the copolymers with f_{DEm} = 10 mol % are also plotted, whose relaxation time distributions are unimodal. The R_h values for the fast mode component observed for the copolymers are within the range of 6−9 nm independent of C_p. The fast mode may be attributed to the translational diffusion of a unimer (single polymer state) or an "oligomeric" micelle (an aggregate of a small number of polymer chains), but we have not so far been able to confirm which is the case. On the other hand, the slow relaxation mode is attributable to polymer-bound $C_{12}E_m$ micelles that are interconnected by polymer chains, i.e., a cross-linked structure. Values of R_h for the slow mode components increase gradually with increasing C_p in a low-C_p region but markedly increase

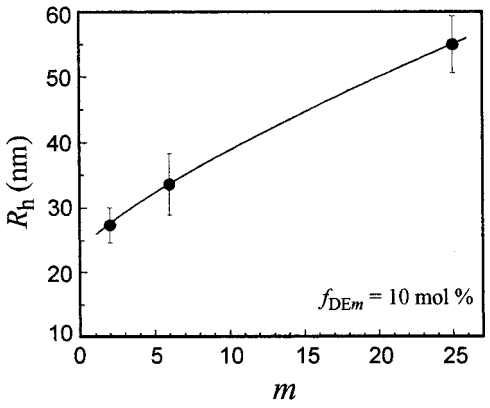

Figure 8. Effect of m on R_h for the copolymers with f_{DEm} = 10 mol % in 0.1 M NaCl aqueous solutions. The error bars include the values with varying C_p from 0.195 to 12.5 g/L.

with C_p in a higher C_p region; i.e., the degree of cross-linking increases gradually with C_p at C_p < 10 g/L but markedly at C_p > 10 g/L. R_h values for the slow mode component for the copolymers with f_{DE6} = 1 and 5 mol % are ca. 75 and 60 nm, respectively, at $C_p \approx 0.78$ g/L. As C_p is increased to 25 g/L, however, R_h values increase to ca. 320 and ca. 285 nm, respectively. In the case of the copolymer with f_{DE6} = 10 mol %, R_h values are much smaller than those for the slow mode for the copolymers with f_{DE6} = 1, 5, and 20 mol %, ranging 35−40 nm in the range of C_p from 0.195 to 12.5 g/L (Figure 7a). R_h values for the copolymer with f_{DE6} = 20 mol % are in the range of 60−370 nm, increasing with increasing C_p.

For the AMPS−DE2MA copolymers with f_{DE2} = 1 and 15 mol %, R_h values are much smaller than those for the AMPS−DE6MA copolymers with f_{DE6} = 1, 5, and 20 mol % (Figure 7), but the dependence of R_h on C_p is qualitatively the same as that for the AMPS−DE6MA copolymers.

The dependence of R_h on the length of the EO spacer for the copolymers with f_{DEm} = 10 mol % is depicted in Figure 8. Since R_h values for these copolymers are virtually independent of C_p over a wide range, we chose the copolymers with f_{DEm} = 10 mol % to show the effect of the spacer length on R_h. As can be seen in Figure 8, R_h increases with increasing m. As discussed earlier, polymer chains are cross-linked through the micelle formation of surfactant side chains, yielding polymer assemblies. We attempted to estimate the number of polymer chains per polymer assembly using SLS, but we were unable to obtain the mass of the polymer assembly because Zimm plots were found to be highly distorted (data not shown) due to the fact that increasing the numbers of polymer chains aggregate with increasing C_p. The values of R_h plotted in Figure 8 correspond to the hydrodynamic radii of the polymer assemblies. The size of the polymer assembly increases as m increases, suggesting that interpolymer association is more favorable for the copolymer with longer EO spacer.

Rheological Behavior of Copolymer Solutions. Zero-shear viscosities (η_0) for the copolymers with f_{DEm} = 10 mol % with varying m in 0.1 M NaCl aqueous solutions are plotted in Figure 9 as a function of C_p over the range 1 g/L ≤ C_p ≤ 100 g/L. In fact, the viscosity values given in Figure 9 are steady shear viscosities measured at a shear rate of 0.01 s^{-1} at which the solutions were confirmed to behave as a Newtonian fluid. Therefore, we regarded these viscosities as η_0. It

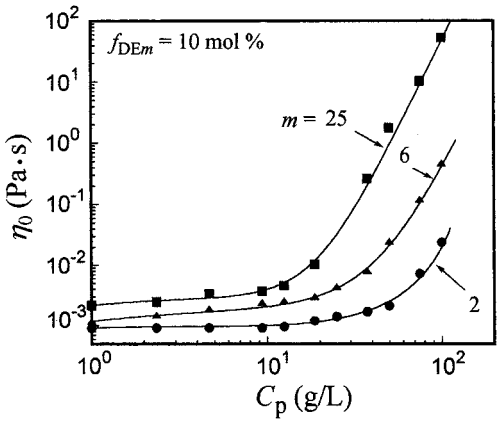

Figure 9. Plots of zero shear viscosity (η_0) at 25 °C for the copolymers with f_{DEm} = 10 mol % in 0.1 M NaCl aqueous solutions as a function of C_p.

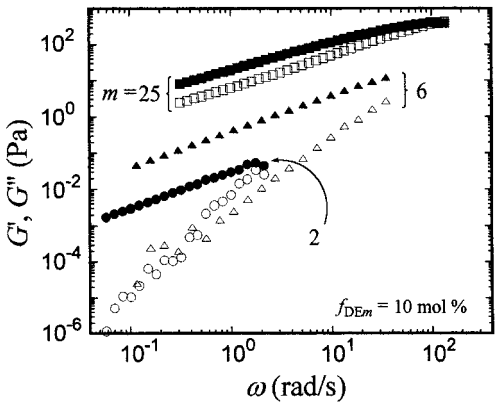

Figure 10. Plots of storage (G') and loss (G'') moduli as a function of angular frequency (ω) for the copolymers with f_{DEm} = 10 mol % at C_p = 100 g/L in 0.1 M NaCl aqueous solutions. Open and closed symbols represent G' and G'', respectively. Shear stress applied is 1.0 Pa at 25 °C.

was found that the viscosities were higher for the copolymer with longer EO spacer at all C_p. This trend is qualitatively consistent with the observation that R_h is larger for the copolymer with longer EO spacer (Figure 8). This is particularly true in a low-C_p region (<10 g/L) where the degree of cross-linking of polymer chains formed through micelle formation is relatively small. The viscosity increases gradually with increasing C_p in the low-C_p region, but it increases more significantly at C_p higher than ca. 15, 25, and 50 g/L for the copolymers with m = 25, 6, and 2, respectively. In these high-C_p regions, the degree of cross-linking increases greatly with increasing C_p, yielding a macroscopic network. The viscosities for the copolymer with m = 25 are roughly 3 and 2 orders of magnitude higher than those for the copolymers with m = 2 and 6, respectively, at C_p > 50 g/L, indicating that the size of the network structure is much larger for the copolymer with longer EO spacer.

Figure 10 shows plots of storage (G') and loss (G'') modulus as a function of angular frequency (ω) for the copolymers with f_{DEm} = 10 mol % with varying m at C_p = 100 g/L in 0.1 M NaCl aqueous solutions. In the case of the copolymers with m = 2 and 6, the solutions behave as a viscoelastic fluid following a single element Maxwell model (i.e., $G' \propto \omega^2$ and $G'' \propto \omega$)[39] over the frequency domains investigated. In the case of the copolymer with m = 25, however, $G'-\omega$ and $G''-\omega$ plots deviate from the Maxwell model. As C_p is increased,

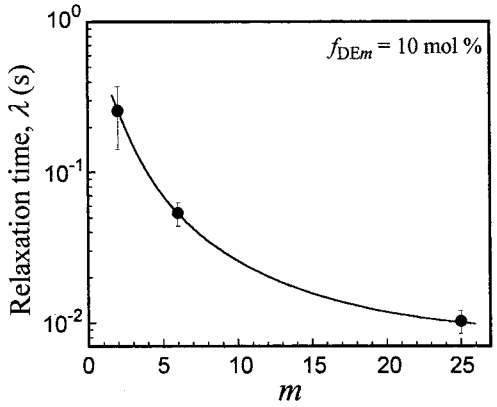

Figure 11. Dependence of the terminal relaxation time on m for the copolymers with f_{DEm} = 10 mol % in 0.1 M NaCl aqueous solutions at 25 °C.

both G' and G'' increase, and they become close to each other, solutions showing significantly elastic properties.[40] The dominant elastic properties arise from a large number of cross-links formed by interpolymer micellization of polymer-bound $C_{12}E_{25}$ moieties. At C_p = 100 g/L, solutions of the copolymer with m = 25 exhibit gel-like behavior.

The time of intersection, λ (= $2\pi\omega^{-1}$), at which G' equals G'', was estimated and plotted against m in Figure 11. For AMPS−DE6MA, λ was estimated by extrapolation. It should be noted here that λ was found to be practically independent of C_p for all the copolymers (data not shown). λ may be regarded as the terminal relaxation time that may be associated with the lifetime of the transient network.[41−43] As clearly seen from Figure 11, the relaxation time decreases markedly with increasing m. This suggests that the lifetime of the transient network is shorter for the copolymers with longer EO spacer. The lifetime of the transient network may depend on the residence time for a polymer-bound surfactant unit in a micelle under shear conditions.

According to a simple theory for transient networks or reversible physical bonds in which the network junctions can break and recombine, the magnitude of G' at a high ω value is related to the number density of mechanically active chains.[40] If we compare G' values at λ, G' for m = 25 is 10 and 10^4 times larger than those for m = 6 and 2, respectively, at C_p = 100 g/L. This indicates that the cross-linking density depends strongly on the length of EO spacer, and the density increases markedly with increasing m.

Discussion

The effects of m and f_{DEm} on the apparent cmc are apparently complex, but the observations in Figure 3a may be explained by the following arguments. In order for the micellization of polymer-bound surfactants to occur through interpolymer associations, an enthalpic penalty caused by an excluded-volume effect among polymer chains should be overcome with the positive entropy (+ΔS) due to hydrophobic associations of alkyl chains. By the insertion of a longer EO spacer, the excluded-volume effect among polymer chains (especially, electrostatic repulsion) on the side-chain micellization becomes smaller.[18] Moreover, since a longer flexible spacer can "decouple" the motions of the main chain and the hydrophobe, the motional and hence geometrical freedom of the hydrophobe at an end of a longer spacer should be larger.[18] These two spacer effects make the copolymer with a longer EO spacer more favorable to undergo side-chain micellization among different polymer chains, thus the copolymer exhibiting a lower apparent cmc. As the hydrophobe content is increased up to ca. 10 mol %, apparent cmc values were found to decrease irrespective of m (Figure 3a). An increase in the surfactant comonomer content makes the surfactant association more favorable, thus leading to a decrease in the apparent cmc. In fact, the interpolymer association occurs competing with intrapolymer association. As shown in the inset of Figure 2, the slope of the plot for $[Py]_m/[Py]_w$ vs C_p below the apparent cmc corresponds to the dissolution of pyrene probes into hydrophobic microdomains with a smaller N_{agg} formed by intrapolymer association. The observation that the copolymer with a higher surfactant comonomer content shows a slightly steeper slope suggests that intrapolymer association is more favorable for the copolymers with higher surfactant comonomer contents. Above 10 mol % surfactant comonomer content, apparent cmc increases with an increase in the comonomer content (Figure 3a). A plausible cause for this observation is that as the content of the surfactant units in the copolymer increases beyond 10 mol %, the polymer-bound surfactants are more prone to associate on the same polymer chain and thus the number of surfactant moieties available for interpolymer association decreases. This may lead to an increase in apparent cmc. An increase in intrapolymer association, as compared to interpolymer association, with increasing hydrophobe content beyond a certain level was observed for another types of hydrophobically modified polyelectrolytes in our previous studies.[12,13,17,44,45] Therefore, this may be a general tendency for water-soluble hydrophobically modified polyelectrolytes.

We previously determined N_{agg} for the AMPS−DE25MA copolymers with f_{DE25} = 10−30 mol % to be 50−70 depending on f_{DE25}.[19] These N_{agg} values are similar to that for the corresponding free surfactant ($C_{12}E_{25}$).[19] As shown in Figure 6 for the AMPS−DEmMA copolymers with a 10 mol % surfactant comonomer content, the increase in m from 2 to 25 leads to a decrease in N_{agg} from 465 ± 50 to 67 ± 5. In the AMPS−DEmMA copolymers with m = 6 and 25, dodecyl groups at an end of the EO spacer are distant enough from the polymer backbone to be able to associate freely with others to form micelle cores whose N_{agg} values are similar to those for the corresponding free $C_{12}E_m$ surfactants. In other words, at $m \geq 6$, there is no or little steric restriction of the polymer backbone on the micellization of side-chain surfactants.

The finding that N_{agg} values for the copolymers with m = 6 and 25 are almost the same as those of the corresponding free surfactants is consistent with the finding that K_v values for pyrene probes between the micellar phase and the water phase are almost the same as those for the free surfactant micelles (Figure 3b). With increasing surfactant comonomer content, K_v increases to a constant level. This indicates that, for the copolymers with low surfactant comonomer contents (<5 mol %), N_{agg} values of the polymer-bound micelles formed above apparent cmc are smaller than those for the copolymers with higher comonomer contents because K_v correlates with the size of the micelle core, i.e., the N_{agg} value. In fact, for the copolymers with f_{DEm} < 5 mol %, pyrene probes (at a concentration of 1×10^{-7} M) could not be dissolved completely into hydrophobic

microdomains even at the highest C_p (50 g/L), and therefore, we were unable to determine N_{agg}. K_v for the copolymer with a longer EO spacer converges to a maximum value at a lower surfactant comonomer content (Figure 3b), suggesting that at low f_{DEm} the copolymer with a larger m forms micelles with a larger N_{agg} because the motions of the polymer chain and hydrophobes are more "decoupled".

The effects of the EO spacer length can also be seen in the size of polymer assemblies, R_h increasing with increasing m (Figure 8). Since the molecular weights and molecular weight distributions of the copolymers are not much different among the polymers used in this study (Table 1), it is obvious that the fraction of surfactant units on the same polymer chain occupying different micelles (i.e., the extent of cross-linking) increases with increasing EO spacer length. This was also supported from the results of viscosity (Figure 9). At any C_p, low shear viscosities are higher for the copolymers with longer EO spacer. From the observations that R_h (Figure 8) and η_0 (Figure 9) increase with increasing m, it is obvious that the extent of interpolymer association, relative to intrapolymer association, increases with increasing m (up to 25).

Tam et al.[24c] reported that, in the case of the terpolymer of sodium methacrylate (56 mol %), ethyl acrylate (42 mol %), and an acrylate substituted with $HO(CH_2CH_2O)_mC_{32}H_{65}$ with varying m (2 mol %), a modified alkali swellable/soluble emulsions (HASE) model polymer, a maximum effect of promoting interpolymer association was achieved when m was more or less 10. According to their results, as m is increased from 10 to 40 in the HASE model polymer, the probability of forming interpolymer aggregates decreases, and in turn the probability of forming intrapolymer aggregates increases.[24c] Therefore, it may be suggested that if we further increase the length of the EO spacer in the AMPS−DEmMA copolymers beyond m = 25, the tendency for intrapolymer association may increase with increasing m at a certain m. On the other hand, Hogen-Esch et al.[18] reported that, in the case of copolymers of acrylamide and an acrylate substituted with a hydrophobe end-capped $(CH_2CH_2O)_m$ group with m ranging from 1 to 3, longer EO spacers were more effective in promoting interpolymer association.[18] The AMPS−DEmMA copolymers in the present study consist of much higher contents of surfactant moieties together with strong electrolyte units, and also the range of the EO spacer lengths investigated is much different, but our results on the effect of the EO spacer length seem to be qualitatively in agreement with their results.

The polyelectrolyte-bound nonionic surfactant micelles are a novel polymer micelle system that may find various applications for practical use. The interest in this novel system is twofold: (i) properties of polymer-bound micelles and (ii) properties of physically cross-linked polymer solutions. The polymer-bound micelles in the present study are very different from conventional free micelles in that (1) all the surfactants are polymer-bound and no free (small molecular) surfactants coexisting, (2) apparent cmc is much lower than that of free surfactants while N_{agg} is about the same (solubilizing ability is expected to be about the same), (3) since all the micelles are interconnected by polymer chains, micelles are brought into very close proximity, thus giving a very high local concentrations of the micelles while retaining their N_{agg} (i.e., size and shape) unchanged, and (4) an array of the micelles acts as a polymer network. On the other hand, solution properties for the polymers cross-linked by micelles are unique in that the dynamic nature of the cross-link can be determined by the dynamic nature of the micelle, thus allowing one to design transiently cross-linked polymer systems with various dynamic properties including stimuli-responsive aqueous polymer systems.

Conclusions

The micellization of nonionic surfactant moieties, $C_{12}E_m$ (where m = 2, 6, and 25), covalently linked to polyAMPS as side chains was investigated by fluorescence, QELS, and rheological techniques in 0.1 M NaCl aqueous solutions. Apparent cmc, N_{agg} of the side-chain hydrophobes in a micelle core, R_h of polymer assemblies, viscosity, and viscoelastic behavior of polymer-bound micelle solutions were investigated as a function of m. Apparent cmc decreased with increasing m. This trend is opposite to that of free $C_{12}E_m$ surfactants. N_{agg} decreased with increasing m, a trend similar to that of the free surfactant molecules, and N_{agg} values for the polymers with m = 6 and 25 were virtually the same as those for free $C_{12}E_6$ and $C_{12}E_{25}$ micelles, respectively. R_h increased with increasing m. Steady-shear viscosity was higher for larger m. Viscosities for the copolymers with m = 25 are roughly 2 and 3 orders of magnitude higher than those of the copolymers with m = 6 and 2, respectively, at a given C_p, indicative of the size of the network of the copolymer being larger for larger m. The number density of mechanically active chains for the polymer with m = 25 is roughly 1 and 4 orders of magnitude larger than those for the polymers with m = 6 and 2, respectively, at a given C_p. The formation of a network structure occurs more favorably for the copolymer with larger m. The rheological terminal relaxation time decreased with an increase in m, indicating that the lifetime of the transient network is shorter for larger m.

Acknowledgment. This work was supported in part by Shorai Foundation for Science and Technology and in part by a Grant-in-Aid for Scientific Research No. 10450354 from the Ministry of Education, Science, Sports and Culture, Japan.

References and Notes

(1) Bock, J.; Varadaraj, R.; Schulz, D. N.; Maurer, J. J. In *Macromolecular Complexes in Chemistry and Biology*; Dubin, P., Bock, J., Davies, R. M., Schulz, D. N., Thies, C., Eds.; Springer-Verlag: Berlin, 1994; p 33 and references therein.
(2) *Polymers as Rheology Modifiers*; Schulz, D. N., Glass, J. E., Eds.; Advances in Chemistry Series 462; American Chemical Society: Washington, DC, 1991.
(3) *Hydrophilic Polymers, Performance with Environmental Acceptance*; Glass, J. E., Ed.; Advances in Chemistry Series 248; American Chemical Society: Washington, DC, 1996.
(4) *Polymers in Aqueous Media: Performance through Association*; Glass, J. E., Ed.; Advances in Chemistry Series 223; American Chemical Society: Washington, DC, 1989.
(5) Hu, Y.; Smith, G. L.; Richardson, M. F.; McCormick, C. L. *Macromolecules* **1997**, *30*, 3526.
(6) Hu, Y.; Armentrout, R. S.; McCormick, C. L. *Macromolecules* **1997**, *30*, 3538.
(7) Kramer, M. C.; Welch, C. G.; Steger, J. R.; McCormick, C. L. *Macromolecules* **1995**, *28*, 5248.
(8) (a) Binana-Limbelé, W.; Zana, R. *Macromolecules* **1990**, *23*, 2731. (b) Binana-Limbelé, W.; Zana, R. *Macromolecules* **1987**, *20*, 1331.
(9) Morishima, Y.; Nomura, S.; Ikeda, T.; Seki, M.; Kamachi, M. *Macromolecules* **1995**, *28*, 2874.

(10) Chang, Y.; McCormick, C. L. *Macromolecules* **1993**, *26*, 6121.
(11) Branham, K. D.; Snowden, H. S.; McCormick, C. L. *Macromolecules* **1996**, *29*, 254.
(12) Yamamoto, H.; Mizusaki, M.; Yoda, K.; Morishima, Y. *Macromolecules* **1998**, *31*, 3588.
(13) Yamamoto, H.; Morishima, Y. *Macromolecules* **1999**, *32*, 7469.
(14) Yusa, S.; Kamachi, M.; Morishima, Y. *Langmuir* **1998**, *14*, 6059.
(15) Noda, T.; Morishima, Y. *Macromolecules* **1999**, *32*, 4631.
(16) Morishima, Y. In *Solvents and Self-Organization of Polymers*; Webber, S. E., Tuzar, D., Munk, P., Eds.; Kluwer Academic Publishers: Dordrecht, The Netherlands, 1996; p 331.
(17) Hashidzume, A.; Yamamoto, H.; Mizusaki, M.; Morishima, Y. *Polym. J.* **1999**, *31*, 1009.
(18) Hwang, F. S.; Hogen-Esch, T. E. *Macromolecules* **1995**, *28*, 3328.
(19) Noda, T.; Hashidzume, A.; Morishima, Y. *Macromolecules* **2000**, *33*, 3694.
(20) Noda, T.; Hashidzume, A.; Morishima, Y. *Langmuir* **2000**, *16*, 5324.
(21) Schultz, D. N.; Kaladas, J. J.; Maurer, J. J.; Bock, J.; Pace, S. J.; Schultz, W. W. *Polymer* **1987**, *28*, 2110.
(22) Kumacheva, E.; Rharbi, Y.; Winnik, M. A.; Guo, L.; Tam, K. C.; Jenkins, R. D. *Langmuir* **1997**, *13*, 182.
(23) Horiuchi, K.; Rharbi, Y.; Spiro, J. G.; Yekta, A.; Winnik, M. A.; Jenkins, R. D.; Bassett, D. R. *Langmuir* **1999**, *15*, 1644.
(24) (a) Tirtaatmadja, V.; Tam, K. C.; Jenkins, R. D. *Macromolecules* **1997**, *30*, 1426. (b) Tirtaatmadja, V.; Tam, K. C.; Jenkins, R. D. *Macromolecules* **1997**, *30*, 3271. (c) Tam, K. C.; Farmer, M. L.; Jenkins, R. D.; Bassett, D. R. *J. Polym. Sci., Part B* **1998**, *36*, 2275.
(25) (a) Dai, S.; Tam, K. C.; Jenkins, R. D. *Macromolecules* **2000**, *33*, 404. (b) Islam, M. F.; Jenkins, R. D.; Bassett, D. R.; Lau, W.; Ou-Yang, H. D. *Macromolecules* **2000**, *33*, 2480.
(26) Vorobyova, O.; Yekta, A.; Winnik, M. A.; Lau, W. *Macromolecules* **1998**, *31*, 8998.
(27) Wilhelm, M.; Zhao, C.-L.; Wang, Y.; Xu, R.; Winnik, M. A.; Mura, J.-L.; Riess, G.; Croucher, M. D. *Macromolecules* **1991**, *24*, 1033.
(28) (a) Infelta, P. P.; Grätzel, M.; Thomas, J. K. *J. Phys. Chem.* **1974**, *78*, 190. (b)Tachiya, M. *Chem. Phys. Lett.* **1975**, *33*, 289. (c) Infelta, P. P. *Chem. Phys. Lett.* **1979**, *61*, 88. (d) Tachiya, M. In *Kinetics of Nonhomogeneous Processes*; Freeman, G. R., Ed.; Wiley & Sons: New York, 1987; pp 575−650.
(29) Yekta, A.; Aikawa, M.; Turro, N. J. *Chem. Phys. Lett.* **1979**, *63*, 543.
(30) (a) Jakeš, J. *Czech. J. Phys.* **1988**, *B38*, 1305. (b) Jakeš, J.; Štěpánek, P. *Czech. J. Phys.* **1990**, *B40*, 972. (c) Štěpánek, P. In *Dynamic Light Scattering*: *The method and some applications*; Brown, W., Ed.; Oxford University Press: New York, 1993; pp 177−241 and references therein.
(31) (a) Nicolai, T.; Brown, W.; Hvidt, S.; Heller, K. *Macromolecules* **1990**, *23*, 5088. (b) Brown, W.; Štěpánek, P. *Macromolecules* **1988**, *21*, 1791.
(32) (a) Selser, J. In *Light Scattering: Principles and development*; Brown, W., Ed.; Oxford University Press: New York, 1996; pp 232−254 and references therein. (b) Nicolai, T.; Brown, W. In *Light Scattering: Principles and Development*; Brown, W., Ed.; Oxford University Press: New York, 1996; pp 166−200 and references therein.
(33) (a) Schätzel, K. In *Dynamic Light Scattering: The method and some applications*; Brown, W., Ed.; Oxford University Press: New York, 1993; pp 76−148 and references therein. (b) Peters, R. In *Dynamic Light Scattering: The method and some applications*; Brown. W., Ed.; Oxford University Press: New York, 1993; pp 149−176 and references therein.
(34) (a) Phillies, G. D. *J. Anal. Chem.* **1990**, *62*, 1049A. (b) Phillies, G. D. *J. Chem. Phys.* **1988**, *89*, 91.
(35) Kalyanasundaram, K.; Thomas, J. K. *J. Am. Chem. Soc.* **1977**, *99*, 2039.
(36) van Os, N. M.; Haak, J. R.; Rupert, L. A. M. *Physico-Chemical Properties of Selected Anionic, Cationic and Nonionic Surfactants*; Elsevier Science: Amsterdam, 1993.
(37) Malliaris, A.; Lang, J.; Sturm, J.; Zana, R. *J. Phys. Chem.* **1987**, *91*, 1475.
(38) Atik, S. S.; Nam, M.; Singer, L. A. *Chem. Phys. Lett.* **1979**, *67*, 75.
(39) Ferry, J. D. *Viscoelastic Properties of Polymers*, 3rd ed.; Wiley & Sons: New York, 1980.
(40) Green, M. S.; Tobolsky, A. V. *J. Chem. Phys.* **1940**, *14*, 80.
(41) Doi, M.; Edwards, S. F. *The Theory of Polymer Dynamics*; Oxford University Press: Oxford, 1986.
(42) (a) Tanaka, F.; Edwards, S. F. *J. Non-Newtonian Fluid Mech.* **1992**, *43*, 247. (b) Tanaka, F.; Edwards, S. F. *J. Non-Newtonian Fluid Mech.* **1992**, *43*, 273. (c) Tanaka, F.; Edwards, S. F. *J. Non-Newtonian Fluid Mech.* **1992**, *43*, 289. (d) Tanaka, F.; Edwards, S. F. *Macromolecules* **1992**, *25*, 1516.
(43) Rubinstein, M.; Dobrynin, A. V. *Trends Polym. Sci.* **1997**, *5*, 181.
(44) Yamamoto, H.; Tomatsu, I.; Hashidzume, A.; Morishima, Y. *Macromolecules* **2000**, 33, 7852.
(45) Suwa, M.; Hashidzume, A.; Morishima, Y.; Nakato, T.; Tomida, M. *Macromolecules* **2000**, *33*, 7884.

MA0017283